Radiation Dose to the Bladder Wall from 2-[^{18}F] Fluoro-2-deoxy-D-glucose in Adult Humans

Michael T. Dowd, Chin-Tu Chen, Michael J. Wendel, Peter J. Faulhaber, and Malcolm D. Cooper

The University of Chicago, Department of Radiology, Chicago, Illinois

Accurate determination of the radiation dose to the bladder wall from 2-[^{18}F]fluoro-2-deoxy-D-glucose (2-[^{18}F]FDG) is important because the bladder is the critical organ in radiotracer studies using 2-[^{18}F]FDG. The radiation dose to the bladder wall from injected 2-[^{18}F]FDG was estimated using both a dynamic bladder model and the conventional MIRD model. The dynamic model takes into account the excretion rate, the varying size of the bladder, the volume at injection, and an estimated bladder time activity curve. Our data from 302 adult subjects in a five-year period indicate that when the bladder is large at the time of injection, the dose to the bladder is greatly reduced. The absorbed dose of the bladder based on the dynamic model for an initial volume of 450 ml is 0.16 ± 0.06 rad/mCi, while that for an initial volume of 200 ml is calculated to be 0.37 ± 0.18 rad/mCi. The MIRD model estimates an average value of 0.35 ± 0.16 rad/mCi for the 302 cases.

J Nucl Med 1991;32:707–712

The use of the radiotracer 2-[^{18}F]fluoro-2-deoxy-D-glucose (2-[^{18}F]FDG) in conjunction with positron emission tomography (PET) has increased tremendously in the past few years. The accurate determination of the radiation absorbed dose is important for the following reasons. First, it allows a more accurate estimate of the radiation risks to volunteers and patients. Second, a more accurate estimate can improve on the calculation for allowable injected dose. The critical organ in 2-[^{18}F]FDG studies is the bladder wall. Early estimates for the radiation absorbed dose to the bladder wall from 2-[^{18}F]FDG have ranged from 0.289 (*1*) to 0.44 (*2*) rad/mCi. These estimates are based on the MIRD model, which assumes a static volume of 200 ml for the bladder. The latter of the two is based on the most current version of the MIRD schema (*3*) for organs with walls; while the former is based on an earlier version of the MIRD model (*4*). Other estimates, based on radioactivity (*5*) distribution data in the dog, have been as low as 0.144 rad/mCi. Actual absorbed doses vary widely depending upon initial bladder volume, urine output, voiding schedule, rate of elimination of the specific radiotracer, and residual amount in the bladder after voiding. A dynamic bladder model that takes these factors into account was developed previously at our institution (*6*).

In the present study, we calculated the radiation absorbed doses to the bladder wall from 2-[^{18}F]FDG based on both the MIRD schema and the dynamic model. This study is based on 302 adult subjects that have participated in various research protocols at this institution from January 1984 to May 1989.

METHODS AND MATERIALS

Human Subjects

Our protocol for ongoing research projects using 2-[^{18}F]FDG requires that the first post-study void from the subject be collected and an aliquot be assayed for ^{18}F activity. In order to be used in this study, a subject must have a complete data set with respect to bladder dose analysis, which includes pre-study void time, first post-study void time, volume of the void, amount of activity in the void, injected dose, and the plasma time-activity curve for 2-[^{18}F]FDG. If for any reason any part of this information was not obtained, the subject was excluded from the present study. Additionally, all subjects included in this study were adults 18 yr of age or older. Of the approximately 500 subjects that have had 2-[^{18}F]FDG PET studies at our research center, 302 were deemed acceptable for this radiation absorbed dose study. It must be noted that some of these are normals and others are patients in various categories (e.g., epileptics, Alzheimer's disease, brain tumor, etc.). No known renal dysfunction was noted in any of the normals or the patients. All subjects signed informed consent forms. Subjects were asked to refrain from eating and drinking (except for water or sugar-free decaffeinated drinks) from midnight the night before the PET study. Arterialized blood samples were taken rapidly during the first 2 min, and at increasing intervals for the duration of the experiment (usually 60 min postinjection). Urine samples were obtained from each patient 35-180 min postinjecton, with the average first void time being 83 min with a standard deviation of 19 min.

Activity Measurements

The 2-[^{18}F]FDG samples for injection, as well as a 3-ml aliquot of the subjects' urine, were measured in a dose calibrator. The 3-ml aliquot of the subjects' urine was used so that the geometry matches the 3-ml injected dose that is given to subjects. The blood samples were centrifuged, 200 μl aliquots of the plasma were added to 1.8 ml of distilled water for assay in a NaI well counter. These data were then used to construct an 2-[^{18}F]FDG plasma time-activity curve.

Received Jun. 1, 1990; revision accepted Oct. 1, 1990.

For reprints contact: Malcolm D. Cooper, MD, University of Chicago, Box 433, FMI, 5841 S. Maryland Ave., Chicago, IL 60637.

Calculation of Urine Flow Rate and Initial Volume

In order to estimate the urine production rate and the bladder volume at injection, the time of last void before the PET study (t_{pre}), the time of first void after the PET study (t_1), the time of 2-[^{18}F]FDG injection (t_{inj}), and the volume of the first poststudy void (V_1) were recorded. It is assumed that the residual volume in the bladder (V_{res}) is the same for each void. Calculation of the urine production rate (R) is then

$$R = \frac{V_1}{t_1 - t_{pre}}, \quad \text{Eq. 1}$$

which will give a result in ml/min. The volume at injection (V_{inj}) can then be calculated by

$$V_{inj} = V_1 - [R(t_1 - t_{inj})] + V_{res}. \quad \text{Eq. 2}$$

A range of residual volumes were used in the calculation of the absorbed dose by the bladder wall.

Generation of Bladder Time-Activity Curve

The decay-corrected plasma time-activity measurements can be fitted with a three-exponential curve P(t) with the units counts/unit time:

$$P(t) = A\exp(-\lambda_1 t) + B\exp(-\lambda_2 t) + C\exp(-\lambda_3 t). \quad \text{Eq. 3}$$

This plasma time-activity curve can then be used to approximate a bladder activity-uptake curve, also decay corrected. (Fig. 1). The bladder activity-uptake curve can be described by a curve that is complementary to the plasma time-activity curve:

$$G(t) = A(1 - \exp(-\lambda_1 t)) + B(1 - \exp(-\lambda_2 t)) + C(1 - \exp(-\lambda_3 t)). \quad \text{Eq. 4}$$

This bladder activity curve has the same form as the integral of the plasma time-activity curve given as Equation 3.

The actual proportion of the injected dose excreted through the bladder can be determined by defining a constant that relates this bladder uptake curve to the urine assay at the first poststudy void as:

$$K = \frac{\%\text{ injected activity at } t_{v1}}{\text{height of time activity curve at } t_{v1}}, \quad \text{Eq. 5}$$

where t_{v1} is the time of the first void. In determining the percent injected activity in the bladder at the time of the first void the residual volume must be taken into account. The factor K can then be used to convert the count data of the bladder time-activity curve to percent injected dose by simple multiplication:

$$H(t) = K[G(t)]. \quad \text{Eq. 6}$$

An "ideal" bladder curve, which was identical in shape for all of the cases, also was used to calculate the bladder doses. This curve was based on those measured by Jones et al. (*2*) using NaI probes held directly over the bladder.

Bladder Dose Calculation: MIRD Method

The MIRD radiation absorbed dose estimates for the bladder are based on a static bladder of 200 ml and a wall of 45 g (*3*). According to MIRD formalism:

$$\text{Dose} = \tilde{A}_{BC}\, S_{(BW \leftarrow BC)} + \tilde{A}_{TB}\, S_{(BW \leftarrow RB)}, \quad \text{Eq. 7}$$

where BW, BC, and RB refer to bladder wall, bladder contents and remainder of the body, respectively. $S_{(BW \leftarrow BC)}$ is the mean absorbed dose by the bladder wall per unit cumulated activity within the bladder; this value is 0.0018 rad/μCi-hr for ^{18}F (*3*). The cumulated activity can be calculated by integration of Equation 6 and correcting for physical decay of ^{18}F. The calculation of the cumulated activity in the total body, $\tilde{A}_{TB}$, is based on the assumption that exclusive of other organs, the total-body uptake, A_{TB}, is 70% or 700 μCi/mCi injected (*2*). It was also assumed that this distribution was present immediately after injection.

The value of $S_{(BW \leftarrow RB)}$ cannot be found in the MIRD literature but is related to the MIRD S value according to the following equation:

$$S_{(BS \leftarrow RB)} = \frac{S_{(BW \leftarrow TB)} - m_{BC} S_{(BW \leftarrow BC)}}{m_{RB}}, \quad \text{Eq. 8}$$

where BW, BC, and RB are defined as before, TB refers to total body, and m_{RB} is the mass of the remainder of the body and is equal to m_{TB} - m_{BC}. The calculated $S_{(BW \leftarrow RB)}$ is 1.59×10^{-5} rad/μCi-hr. The validity of this approach has been discussed by several authors (*7–9*).

Equation 7 does not take into account the increased radiation dose to the bladder wall due to additional accumulation of activity after the first void and the residual amount of activity that

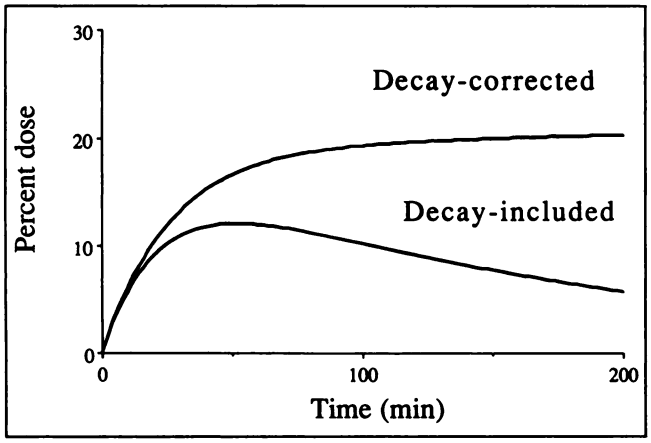

FIGURE 1. Calculated bladder time-activity curves decay-corrected and decay-included.

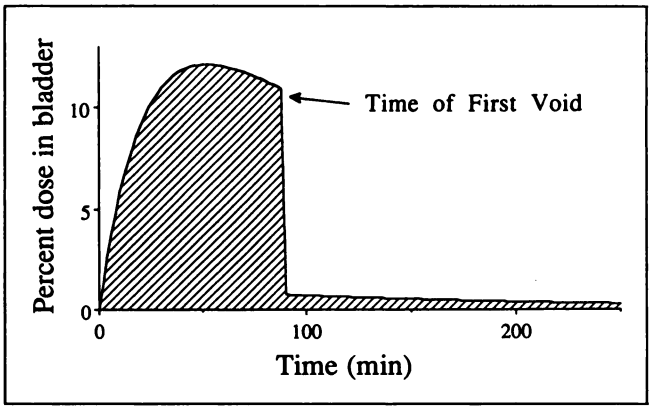

FIGURE 2. The percentage dose in the bladder is shown as a function of time. Shaded area represents the total cumulative activity in the bladder. Residual volume is assumed to be 50 ml.

TABLE 1
Radiation Dose to the Bladder Wall from 2-[^{18}F]FDG

	Residual in bladder			
	10 ml	25 ml	50 ml	100 ml
	(estimated dose to bladder wall in rad/mCi)			
Dynamic Model				
Three-expontential	0.50 ± 0.58	0.46 ± 0.44	0.41 ± 0.35	0.35 ± 0.25
Ideal	0.47 ± 0.41	0.43 ± 0.32	0.38 ± 0.26	0.31 ± 0.22
MIRD Model				
Three-exponential	0.32 ± 0.14	0.33 ± 0.15	0.35 ± 0.16	0.37 ± 0.17
Ideal	0.27 ± 0.11	0.28 ± 0.12	0.30 ± 0.12	0.34 ± 0.14

remains in the bladder after subsequent voids (Fig. 2). This can be resolved by assuming subsequent void times, t_{Vi}, and calculating a residual fraction, f_i, of radioactivity remaining in the bladder at these times. The general equation for the total cumulated activity in the bladder is then:

$$\tilde{A}_{BC} = \int_0^{t_{V1}} H(t)\exp(-\lambda_p t)\,dt + \sum_{i=2}^{n}\left[\int_{t_{V(i-1)}}^{t_{Vi}} H(t)\exp(-\lambda_p t)dt + f_i\tilde{A}_{(i-1)}\right], \quad \text{Eq. 9}$$

where $\tilde{A}_{(i-1)}$ is activity in the bladder at the time of the $(i-1)^{st}$ void. The residual fraction, f_i, is based on residual volumes of 10-100 ml and is equal to the residual volume divided by the total volume in the bladder at void V_i. Subsequent void times every 180 min up to 24 hr were used in our calculations and it was found that the amount of cumulated activity after the third void is negligible.

Bladder Dose Calculation: Dynamic Method

The dynamic model approximates the bladder as a sphere that is increasing in size according to the calculated urine flow rate. According to this dynamic model, the total radiation absorbed dose to the inner surface of the bladder wall due to both penetrating (D_p) and non-penetrating (D_{np}) radiation is given by:

$$D_{np+p}(t) = \int [D_p(t) + D_{np}(t)]\,dt = \frac{1}{60}\int\left[\frac{3.9\ 10^{-3}\,\Gamma A(t)}{V(t)^{2/3}} + \frac{\Delta_\beta A(t)}{2V(t)}\right]dt \quad \text{Eq. 10}$$

where A(t) is the activity in the bladder at time t, V(t) is the volume of the bladder at time t, Γ is the gamma-ray dose rate constant, and Δ_β is an equilbrium dose constant. For ^{18}F, Γ is 6.0 cm^2-rads/μCi-hr[10] and Δ_β is 0.516[11]. The derivation of Equation 10 can be found in reference 6.

As in the MIRD model, the dose to the bladder from the rest of the body must be taken into account; this is done in the identical manner as shown in Equations 7 and 8. The additional bladder activity from post-void accumulation and residual activity in the bladder must also be taken into account. This is analagous to Equation 9. However, with subsequent voids V(t) must be adjusted accordingly. The calculated of V(t) for the n^{th} void after injection is:

$$V_n(t) = V_{res} + R(t_n - t_{(n-1)}), \quad \text{Eq. 11}$$

where $V_n(t)$ is the volume as a function of time for the n^{th} void after injection, V_{res} is the residual volume, t_n is the time of the n^{th}

TABLE 2
Radiation Dose by Bladder Size at Injection

Approximate bladder size (ml)	n	Dynamic* dose (rad/mCi)	Dynamic* stdev	MIRD* dose (rad/mCi)	MIRD* stdev
75	36	0.93	0.49	0.39	0.21
125	64	0.55	0.34	0.33	0.17
175	54	0.40	0.19	0.33	0.13
225	40	0.34	0.18	0.33	0.14
275	32	0.26	0.13	0.31	0.15
325	23	0.21	0.08	0.33	0.13
375	17	0.16	0.07	0.27	0.08
450	15	0.16	0.06	0.30	0.10
550	21	0.14	0.05	0.35	0.13

* 50 ml residual in bladder assumed; see text for details of the calculations.

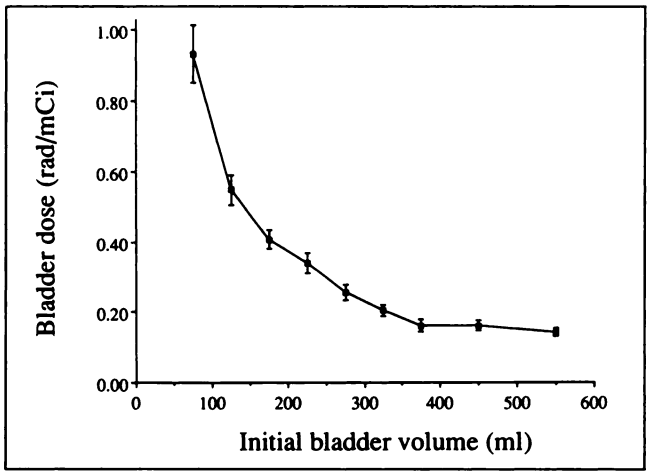

FIGURE 3. Bladder dose as a function of initial bladder volume. Error bars represent s.e.m.

TABLE 3
Various Parameters of Subjects by Groups

	All subjects	Non-hydrated*	Hydrated†
n	302	241	61
Estimated dose dynamic (rad/mCi)	0.41 ± 0.35	0.46 ± 0.41	0.28 ± 0.20
Estimated dose MIRD (rad/mCi)	0.35 ± 0.16	0.35 ± 0.16	0.26 ± 0.06
Bladder volume at injection (ml)	235 ± 140	228 ± 138	260 ± 140
Calculated urine production rate (ml/min)	1.36 ± 1.1	1.19 ± 0.91	2.07 ± 1.5
Time from injection to first void (min)	83 ± 19	87 ± 20	70 ± 10
Bladder volume at time of first void (ml)	290 ± 200	280 ± 185	350 ± 220
Percent injected dose	15 ± 6	16 ± 7	13 ± 3

* Those subjects not drinking water just prior to injection (see text).
† Those subjects asked to drink 250 ml of water just prior to injection (see text).

void in minutes, $t_{(n-1)}$ is the time of the $(n-1)^{st}$ void in minutes, and R is the urine production rate in ml/min.

RESULTS

The radiation absorbed doses of the bladder wall were calculated according to differing residual volumes of urine (10, 25, 50, 100 ml) remaining in the bladder after a void and the results are summarized in Table 1. Using the dynamic model, the estimated dose for someone retaining 100 ml of urine in their bladder is about 30% lower than someone retaining only 10 ml (0.35 versus 0.50 rad/mCi). The calculation based on the MIRD model yields results of 0.32 and 0.37 rad/mCi for those retaining 10 and 100 ml of urine in their bladder.

MIRD Formalism Versus Dynamic Model

Our results indicate that when using estimates based on the dynamic model at low initial bladder volumes the dose to the bladder is greatly increased. When the initial bladder volume is approximately 75 ml the estimated dose to the bladder based on the dynamic model is 0.93 rad/mCi, while those subjects with an initial bladder volume of 550 ml received an estimated 0.14 rad/mCi. The MIRD method yields an average result of 0.39 and 0.35 rad/mCi for those subjects whose bladder volumes at injection, were calculated to be 75 and 550 mls, respectively. The calculation of the bladder dose as a function of bladder size at injection is shown in Table 2. As is expected, the MIRD estimates do not vary with bladder size. Figure 3 shows the relationship between the dynamically estimated bladder dose as a function of bladder size at injection.

Hydrated Versus Nonhydrated

Table 3 also has a breakdown according to the "hydration" status of the subjects. Sixty-one of our subjects were asked to drink approximately 250 ml of water in a 10-min span 15 min prior to injection. The hydrated group started with slightly larger bladders than the non-hydrated group (260 ± 140 ml versus 230 ± 140 ml), their urine flow rates were much higher (2.1 ± 1.5 versus 1.2 ± 0.9 ml/min), and the average time interval between injection and void for the hydrated group was 17 min shorter than the non-hydrated group (70 ± 10 versus 87 ± 20 min). The dynamically estimated bladder doses for the hydrated group were much lower than the nonhydrated group (0.28 ± 0.20 versus 0.46 ± 0.41 rad/mCi). The MIRD radiation absorbed dose estimates were also lower in the hydrated group as compared to the non-hydrated group (0.26 ± 0.06 versus 0.35 ± 0.16 rad/mCi).

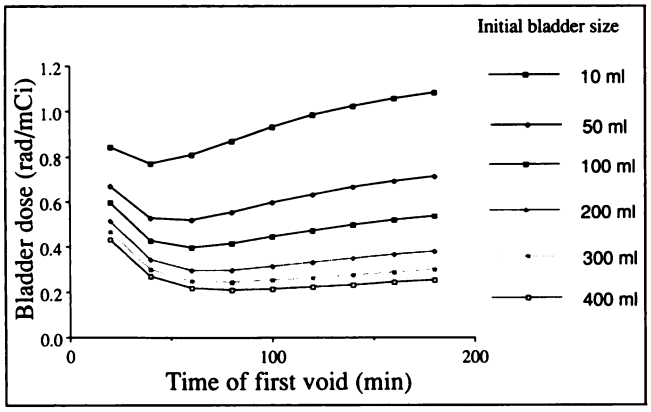

FIGURE 4. Absorbed dose as a function of first void plotted for six bladder volumes. Doses estimated using a dynamic bladder model.

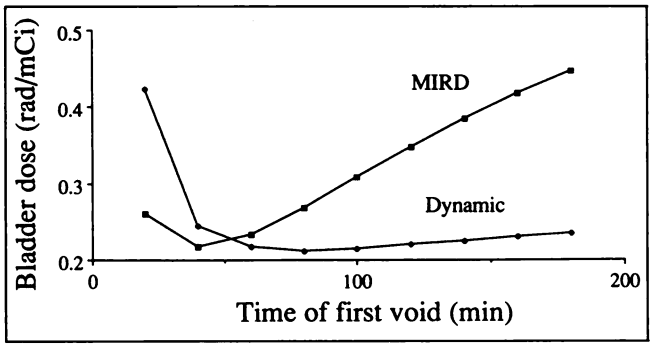

FIGURE 5. Comparison of bladder doses calculated by using a dynamic bladder model and the MIRD model.

DISCUSSION

As stated earlier, two methods for determining the bladder time-activity curves were used to estimate the bladder radiation dose. As seen in Table 2, they give comparable results. The fact that these results do not vary to a large degree suggests that an exact determination of a bladder time-activity curve is not extremely important to the calculation of the dose to the bladder wall from the bladder contents. It seems that a standard bladder time-activity curve will give reasonable results. The factors that play the largest role in the calculation of the dose to the bladder wall using the dynamic method are urine production rate, initial bladder volume, and the residual volume in the bladder after voiding.

MIRD Formalism Versus Dynamic Model

These two methods give comparable estimates for the bladder dose, however, the dynamic model uses a more accurate description of the bladder. The MIRD results presented here compare favorably with those presented by Jones et al. (*2*). In that work, the average dose to the bladder wall was estimated to be 0.44 rad/mCi for a void time of 2 hr. For a void time of 84 min (average void time in this study), the estimated bladder dose in the Jones study would be approximately 0.31 rad/mCi, which is in good agreement with the 0.35 rad/mCi estimated using the MIRD model in the 302 subjects in this study.

Hydrated Versus Nonhydrated

As shown in Table 3, the group of subjects given 250 ml of water just prior to the injection of 2-[^{18}F]FDG had greatly reduced doses to the bladder, as estimated with both the dynamic and the MIRD models. The differences in the dynamically estimated bladder dose can be attributed to the increased urine production rate, the increased initial bladder size, and to a lesser extent, the diminished time of first void of the hydrated group. The decreased dose as calculated by the MIRD model can be attributed mostly to the decreased time of first post-study void. These results suggest that a rapid urine production rate as well as a large initial bladder size are the most important factors in reducing the dynamically calculated absorbed dose of the bladder wall. The voiding schedule does play a role, although it is much more important in the MIRD calculations of the bladder absorbed dose.

Recommendations for Reduction of Dose to the Bladder Wall

Using the dynamic model, in order to minimize the bladder wall dose, subjects should start with their bladders as full as reasonably possible, have a high urine production rate, and void 70–90 min postinjection. As seen in Figure 4, the time of first void yielding the lowest estimated dose varies with the bladder size at the time of injection. Figure 5 shows the effect of varying the voiding schedule on the absorbed dose, where the initial bladder volume is 250 ml, urine production rate is 1.25 ml/min, and 15% of the injected activity accumulates in bladder by the time of the first post-study void, and a 50-ml residual volume is assumed. Second and third void times of 180 and 360 min post-first void were used. The MIRD model estimates that the lowest dose would occur with an initial void of 40 min whereas the lowest dose with the dynamic model is achieved with an initial void time of 80 min. With the MIRD model, voiding after 40 min increases the dose linearly, while the dynamic model predicts very little increase in bladder dose with an increase in time of initial void past 80 min. Neither of the models allows for a minimal radiation absorbed dose if the patient voids as soon as possible after injection, although the MIRD model would allow this if subsequent voids are frequent, rather than being spaced at 3-hr intervals.

CONCLUSIONS

As the use of the radiotracer 2-[^{18}F]FDG increases, the importance of the accurate determination of the radiation absorbed dose of the critical organ, the bladder, is paramount. The MIRD model does not allow for inclusion of all of the parameters that will affect the actual dose to the bladder. The dynamic model used in this study takes these factors into account and gives a much more accurate estimation of the bladder dosimetry, which allows for the determination of voiding schedules that provide the lowest possible dose to the bladder. Using the dynamic method, the lowest radiation dose to the bladder is achieved when the initial bladder volume is large, the urine production rate is high, and the first void is about 80 min postinjection. Reduction in the radiation absorbed dose by following these recommendations may result in an increased number of studies allowable for each subject, thereby making certain types of protocols that require multiple studies more feasible.

ACKNOWLEDGMENTS

This work was supported by DOE grant DE-FG02-86-ER60438. Preliminary results of this work were presented at the 36th Annual Meeting of The Society of Nuclear Medicine, June 1989, St. Louis, Missouri.

REFERENCES

1. Reivich M, Kuhl D, Wolf A, et al. The [^{18}F]fluorodeoxyglucose method for the measurement of local cerebral glucose utilization in man. *Circ Res* 1979;44:127–137.
2. Jones SC, Alavi A, Christman D, Montanez I, Wolf AP, Reivich M. The radiation dosimetry of 2-[F-18]fluoro-2-deoxy-D-glucose in man. *J Nucl Med* 1982;23:613–617.
3. Snyder WS, Ford MR, Warner GG, et al. "S" absorbed dose per unit cumulated activity for selected radionuclides and organs. *MIRD pamphlet 11*. New York: Society of Nuclear Medicine; 1975.
4. Snyder WS, Fisher HL, Warner GG, et al. Estimates of absorbed fractions for monoenergetic photon sources uniformly distributed in various organs of a heterogeneous phantom. MIRD Pamphlet 5. 3. *J Nucl Med* 1969;(suppl 3):7–52.
5. Brownell GL, Ackerman RH, Strauss HW, et al. Preliminary imaging results with ^{18}F-2-fluoro-2-deoxy-D-glucose. *J Comput Assist Tomogr* 1980;4:473–477.

6. Chen CT, Harper PV, Lathrop KA. A simple dynamic model for calculating radiation absorbed dose to the bladder wall. *Proceedings of the fourth international radiopharmaceutical dosimetry symposium, Oak Ridge.* Conf-851113-(DE86010102), 1985:587–612.
7. Smith T. The radiation dosimetry of 2-[F-18]fluoro-2-deoxy-D-glucose in man [Letter] *J Nucl Med* 1980;24:447–448.
8. Cloutier RJ, Watson EE, Rohrer RH, et al. Calculating the radiation dose to an organ. *J. Nucl Med* 1973;14:53–55.
9. Roedler HD, Kaul A. Dose to target organs from remaining body activity: results of the formally exact and approximate solution. In: *Radiopharmaceutical dosimetry symposium—Proc. Conf. Oak Ridge.* Rockville, MD: HEW Publication (FDA), 76-8044;1976:155–162.
10. Loevinger R, Holt JG, Hine GJ. Internally administered radioisotopes. Radiation dosimetry In: Hine GJ, Brownell GL, eds. *Radiation dosimetry.* New York: Academic Press; 1956:801–896.
11. Dillman LT. Radionuclide decay schemes and nuclear parameters for use in radiation-dose estimation. *MIRD Pamphlet* 4. New York: Society of Nuclear Medicine;1969.

15 30

Selected manuscripts from the issues of *The Journal of Nuclear Medicine* published 15 and 30 years ago.
Edited by F.F. Mand

SPRING 1976

Design and Performance Characteristics of a Whole-Body Positron Transaxial Tomograph

Edward J. Hoffman, Michael E. Phelps, Nizar A. Mullani, Carol S. Higgins, and Michel M. Ter-Pogossian

We have designed, built, and tested a device that allows the reconstruction of transaxial tomographic images of the distribution of positron-emitting radiopharmaceuticals in the human head and torso. This is the third in a series of devices that we call positron-emission transaxial tomographs (PETT). The PETT III can measure quantitatively the distribution of any positron-emitting radiopharmaceutical in a cross-sectional slice of the human body. This paper presents: (a) a description of clinically useful PETT; (b) a report on its capabilities in terms of resolution, accuracy, and efficiency; and (c) documentation of the imaging capability of PET III with both patients and volunteers.

Phantom Studies

A uniformity phantom, consisting of a 25-cm diameter by 5-cm deep plexiglas container filled with a ^{68}Ga solution, was scanned with PETT III. The shadow shields were in place and the discriminators set at 100 keV. The distribution of the activity values per pixel in a 15-cm diameter central region of the image was used to evaluate their standard deviation over the field in the reconstructed image: it was found to be ±7.5% of the mean value. The theoretical error for this image, assuming only statistical error, is ±5.3%. Another plexiglas phantom was also imaged to evaluate the quantitative recovery of information in a PETT III image. Within statistical error, the value of the hot spot in the reconstructed image is twice that of the main body and the cold spot is zero.

Initial Patient Studies

A patient with a 2-wk-old cerebral infarct was studied with $^{13}NH_3$, ^{68}Ga-EDTA, and ^{11}CO. The shadow fields were removed to maximize the counting rate. The patient was administered 8 mCi of each of the first two radiopharmaceuticals and 20 mCi of ^{11}CO by inhalation. The images required 8-20 min per slice (20 min for ^{68}Ga), with about 10^6 counts per image. The infarct was prominent in the $^{13}NH_3$ image, while the ^{68}Ga and EMI scans indicated abnormalities adjacent to the actual infarct due to impairment of the blood-brain barrier.

Conclusions

The initial patient studies showed great potential for clinical imaging. The depth-independent resolution, quantitative recovery of radiopharmaceutical distributions, and removal of superimposition of structures give PETT III advantages not present in conventional nuclear medicine imaging systems. With the development of better radiopharmaceuticals, the PETT III system should be able to give better images in shorter times at lower doses. ■

SPRING 1961

From an abstract submitted for the 8th Annual Meeting of The Society of Nuclear Medicine

The Future of Nuclear Medicine

John McAfee

Despite considerable interest during the past decade, radioisotopes used both diagnostically and therapeutically have failed to create a sizable impact upon the practice of medicine. Many large institutions continue to regard radioisotope laboratories as a research luxury rather than as a necessity for good patient care. Within the next decade, this attitude will probably change drastically, as the gap narrows between nuclear physics and instrumentation and their medical applications. The use of radioisotopes in clinical research will parallel the impact of radiotracers on basic biochemistry. The role of radioactive tracers in clinical medicine of the future will probably become equal in importance to that of x-ray diagnosis and therapy.

For nuclear medicine to live up to these expectations, many difficulties in present day practice must be overcome. Laboratories must develop additional facilities designed solely for the training of personnel. Full-time professional staffs must devote more time to adequate training of physicians. Radionuclides and labeled compounds available for the physician's use, currently quite limited in number, must be increased in number. The present day instrumentation facilities of most laboratories include only a few types of gamma detectors. Other instruments will be required to permit the use of a wide variety of compounds labeled with beta emitters in diagnostic studies. The rapid advances in instrumental design may reach a plateau in the years ahead, but the era of radiochemistry as applied to medical problems has just begun. ■